

# Upper Limits on the 21 cm Power Spectrum at $z = 5.9$ from Quasar Absorption Line Spectroscopy

Jonathan C. Pober,<sup>1\*</sup> Bradley Greig,<sup>2</sup> and Andrei Mesinger<sup>2</sup>

<sup>1</sup>*Department of Physics, Brown University, Providence, RI 02912, USA*

<sup>2</sup>*Scuola Normale Superiore, Piazza dei Cavalieri 7, I-56126 Pisa, Italy*

Accepted 2016 August 1. Received 2016 July 11; in original form 2016 10 May

## ABSTRACT

We present upper limits on the 21 cm power spectrum at  $z = 5.9$  calculated from the model-independent limit on the neutral fraction of the intergalactic medium of  $x_{\text{HI}} < 0.06 + 0.05 (1\sigma)$  derived from dark pixel statistics of quasar absorption spectra. Using 21CMMC, a Markov chain Monte Carlo Epoch of Reionization analysis code, we explore the probability distribution of 21 cm power spectra consistent with this constraint on the neutral fraction. We present 99 per cent confidence upper limits of  $\Delta^2(k) < 10$  to  $20 \text{ mK}^2$  over a range of  $k$  from 0.5 to  $2.0 \text{ hMpc}^{-1}$ , with the exact limit dependent on the sampled  $k$  mode. This limit can be used as a null test for 21 cm experiments: a detection of power at  $z = 5.9$  in excess of this value is highly suggestive of residual foreground contamination or other systematic errors affecting the analysis.

**Key words:** dark ages, reionization, first stars – intergalactic medium – galaxies: high-redshift – cosmology: theory – cosmology: observations

## 1 INTRODUCTION

Observations of the highly redshifted 21 cm line of neutral hydrogen have become recognized as one of the most promising probes for exploring the early universe. A particular focus of early experiments is to detect the spatial power spectrum of this emission from the Epoch of Reionization (EoR), where the contrast between neutral and ionized regions of the intergalactic medium (IGM) can produce a relatively strong signal. Several experiments have conducted lengthy observation campaigns with the goal of making a first detection, including the Giant Metre-Wave Radio Telescope (GMRT; Swarup et al. 1991)<sup>1</sup>, the LOw Frequency ARray (LOFAR; van Haarlem et al. 2013)<sup>2</sup>, the Murchison Wide-field Array (MWA; Tingay et al. 2013)<sup>3</sup>, and the Donald C. Backer Precision Array for Probing the Epoch of Reionization (PAPER; Parsons et al. 2010)<sup>4</sup>. To date, only upper limits have been placed on the cosmological signal, with the best constraints coming at  $z = 8.4$  from PAPER (Ali et al. 2015). While not sensitive enough to detect the most generic reionization signals, these measurements were able to place lower limits on the IGM temperature of  $\sim 10 \text{ K}$ , beginning

to rule out some models of “cold reionization” (Pober et al. 2015; Greig et al. 2016).

As these experiments continue to collect data and improve analysis techniques, the possibility of a first detection of the 21 cm signal seems near. A first detection, however, will likely be of low to moderate significance and limited to a narrow range of redshifts and Fourier  $k$  modes. And, nearly all of the upper limits published to date have seen systematic biases that are not consistent with noise (Parsons et al. 2014; Jacobs et al. 2015; Ali et al. 2015; Dillon et al. 2015; Trott et al. 2016). It is therefore exceedingly germane to ask the question: how can one distinguish an early, low-significance 21 cm detection from systematics caused by foregrounds or other instrumental effects?

There are several features intrinsic to the cosmological 21 cm signal that could be used to distinguish it from foregrounds. One of the most commonly proposed is to observe the “rise and fall” of the 21 cm signal with frequency. The hydrogen signal is predicted to peak when the ionization fraction of the IGM is 50 per cent (Lidz et al. 2008; Bittner & Loeb 2011) or somewhat thereafter depending on the relative efficiency of X-ray heating and UV reionization (Mesinger et al. 2013, 2016); therefore, a cosmological signal should show a peak in the power spectrum as a function of redshift (and therefore a peak as a function of frequency, since observed frequency corresponds to redshift of the 21 cm line). Foregrounds on the other hand are dominated by synchrotron emission, which smoothly increases in power to

\* E-mail: Jonathan\_Pober@brown.edu

<sup>1</sup> <http://gmrt.ncra.tifr.res.in/>

<sup>2</sup> <http://www.lofar.org/>

<sup>3</sup> <http://www.mwatelescope.org/>

<sup>4</sup> <http://eor.berkeley.edu/>

wards lower frequencies.<sup>5</sup> However, prospects for detecting this peak are perhaps more limited than initially expected: due to the steep increase of sky noise towards lower frequencies ( $T_{\text{sky}} \propto \nu^{-2.55}$ ), the uncertainties on higher redshift 21 cm measurements grow rapidly, limiting the significance with which an actual rise-and-fall can be detected (Pober et al. 2014). While a decline in signal strength towards lower frequencies can be detected with high significance, the same spectral behavior is shared with foregrounds; therefore, the peak in frequency is the clear discriminant. Moreover, if inhomogeneous recombinations play an import role in the reionization process, they can decrease the power on large scales and reduce the prominence of the peak versus redshift, resulting in a redshift evolution of the cosmological signal that can be more modest than initially predicted, (Sobacchi & Mesinger 2014).

Another potential discriminator could be the (nearly) spherically symmetric shape of the 21 cm signal in  $k$  space, since foregrounds have drastically different angular and spectral properties. However, first generation experiments do not have the sensitivity to measure high- $k$  transverse modes of the power spectrum, so this spherical symmetry will be very difficult to detect (Pober 2015). The shape of the spherically averaged 1D 21 cm power spectrum is itself relatively featureless, with exception of a “knee” on very large scales. Foregrounds are most problematic on these scales, although it may be possible to recover this feature in some cases (Greig & Mesinger 2015). Its usefulness as a robust indicator of a cosmological signal may be limited for first-generation experiments.

Cross-correlation studies present another promising tool for confirming the presence of cosmological emission in 21 cm data. If the signal is truly of cosmological origin, then it should spatially correlate with other tracers of large scale structure, including galaxies and Lyman- $\alpha$  emitters (Furlanetto & Lidz 2007; Sobacchi et al. 2016; Vrbancic et al. 2016), the near infrared background (Wyithe et al. 2007; Fernandez et al. 2014; Mao 2014), and “intensity maps” of other spectral lines such as CO and CII (Gong et al. 2011; Lidz et al. 2011; Gong et al. 2012). However, these correlation studies either require larger volume surveys than are possible with existing instruments or new, dedicated experiments in the case of intensity mapping.

The goal of this letter is to propose and quantify a potential test for the robustness of a purported initial 21 cm detection. It has been recognized that observations at redshifts *after* the end of reionization might provide a null result. It is the contrast between the neutral regions and ionized bubbles within the IGM that leads to large spatial fluctuations in the hydrogen signal, and therefore a relatively bright power spectrum during reionization. Once the IGM is completely ionized, this contrast disappears, and hence the signal becomes undetectable.<sup>6</sup> In this work, we turn this

expectation into a quantitative prediction for the maximum possible brightness of the 21 cm power spectrum at  $z = 5.9$ . This particular redshift is especially useful for these studies, as it falls within the range accessible to current 21 cm experiments, but also has significant observations at other wavelengths that allow for a non-trivial constraint on the 21 cm power. To perform this calculation, we use the model-independent constraint on the neutral fraction at this redshift from McGreer et al. (2015). By measuring the fraction of dark (i.e. zero flux) pixels in the Lyman- $\alpha$  and Lyman- $\beta$  forests in the spectra of high- $z$  quasars, they place a limit on the neutral fraction  $x_{\text{HI}} < 0.06 + 0.05 (1\sigma)$  at  $z = 5.9$ . This technique does not make assumptions about whether dark pixels are caused by genuine cosmic HI regions from an incomplete reionization, or from residual neutral hydrogen in the ionized IGM (note that trace amounts of HI, at the level of  $10^{-4}$ , are sufficient to saturate the Lyman- $\alpha$  forest). Hence, it is a conservative limit, but avoids model-driven assumptions. To turn this constraint into a limit on the 21 cm power spectrum, we use the 21CMMC (Greig & Mesinger 2015)<sup>7</sup> EoR analysis code to perform a Markov chain Monte Carlo (MCMC) exploration of possible 21 cm power spectra given this neutral fraction limit.

The structure of this letter is as follows. In §2, we describe the modeling of the 21 cm power spectrum performed by 21CMMC. In §3, we present the resultant power spectrum limits. We discuss the implications of this result in §4 and conclude in §5. Unless otherwise stated, we assume a  $\Lambda$ CDM cosmological model with the Planck 2015 cosmological parameter values:  $h = 0.6781$ ,  $\Omega_M = 0.308$ ,  $\Omega_b = 0.0484$ ,  $\Omega_{DE} = 0.692$ , and  $\sigma_8 = 0.8149$  (Planck Collaboration et al. 2015).

## 2 POWER SPECTRUM MODELING

21CMMC is an MCMC sampler of 21cmFAST<sup>8</sup>, a semi-numerical simulation code for quickly generating realizations of the ionization history of the universe and associated 21 cm signal. We highlight the relevant details of each code here, but refer the reader to Greig & Mesinger (2015) for more details about 21CMMC and to Mesinger & Furlanetto (2007) and Mesinger et al. (2011) for a complete description of 21cmFAST.

21cmFAST generates IGM density, velocity, source, and ionization fields by creating a realization of the 3D linear density field within a cubic volume and evolving it following the Zel’dovich approximation (Zel’dovich 1970). The ionization field is estimated by applying the excursion set approach of Furlanetto et al. (2004), which compares the time-integrated number of ionizing photons to the number of baryons within regions of decreasing radius, to perturbed 3D density fields. These formalisms and approximations allow for rapid generation of simulated 21 cm cubes (of order 45 seconds for a single redshift realization). When compared with more rigorous simulations, 21cmFAST has been shown to produce power spectra accurate to within 10 to 30 per

<sup>5</sup> While many sources do show a turnover in their synchrotron spectra due to self-absorption, this typically happens at much lower frequencies than the 100 – 200 MHz range where one might expect to see a reionization signal.

<sup>6</sup> While neutral hydrogen still remains in shelf-shielded structures (i.e. galaxies), this signal is orders of magnitude fainter than the signal during reionization (Barkana & Loeb 2007; Crociani et al. 2011; Ansari et al. 2012; Sobacchi & Mesinger 2014). The reason

this signal could be detectable at lower redshifts (e.g.  $z \sim 1$ ) is because of the significant decrease in the brightness of foregrounds and the system noise at higher frequencies (Pober et al. 2013).

<sup>7</sup> <https://github.com/BradGreig/21CMMC>

<sup>8</sup> [http://homepage.sns.it/mesinger/DexM\\_21cmFAST.html](http://homepage.sns.it/mesinger/DexM_21cmFAST.html)

cent on the scales of interest for reionization. The dominant uncertainties come from the ionization field; the underlying matter power spectra agree with N body simulations to better than the per cent level (Mesinger et al. 2011).

The primary physics of reionization are described in 21cmFAST with three key parameters:  $\zeta$ , an ionizing efficiency which converts baryonic mass into a number of ionizing photons;  $T_{\text{vir,min}}$ , a minimum virial temperature below which halos do not produce ionizing photons; and  $R_{\text{mfp}}$ , the maximum horizon of ionizing photons through ionized regions of the IGM.<sup>9</sup> Although this three parameter model is an oversimplification of reionization physics, it provides a physically-motivated basis set for sampling 21 cm power spectra during the EoR, which is the primary requirement for this work. Moreover, the resulting 21 cm power spectra from this simple model agree with those from complex semi-analytical models when using a comparable average halo mass of reionization galaxies (Geil et al. 2015). In this simulation, we use a box of 500 Mpc on a side with  $256^3$  voxels. Note that we do not calculate spin temperature fluctuations in our 21cmFAST simulations, as the spin temperature of the IGM is very likely well above the Cosmic Microwave Background (CMB) temperature at  $z = 5.9$ ;<sup>10</sup> in this limit, the 21 cm signal is independent of the spin temperature.

21CMC uses MCMC sampling to explore the likelihood for the three EoR parameters  $\zeta$ ,  $T_{\text{vir,min}}$ , and  $R_{\text{mfp}}$  (generating a 21mFAST realization for each set) given power spectrum measurements from a 21 cm experiment. Here, we use a modified version of the code, as we do not have power spectrum measurements to compare with. Rather, we explore combinations of EoR parameters that recover neutral fractions consistent with the McGreer et al. (2015) limits at  $z = 5.9$ . This limit is not enough to place significant constraints on any of the three EoR parameters (Greig and Mesinger, in prep.); however, it does place significant constraints on the maximum allowable amplitude of the 21 cm power spectrum. It is this limit that we explore in this work.

### 3 RESULTS

Using 21CMC, we explore the likelihood function for the amplitude of the 21 cm power spectrum using the McGreer et al. (2015) limit and uniform priors on the EoR parameters over the ranges  $5 \leq \zeta \leq 200$ ,  $10^4 \text{ K} \leq T_{\text{vir,min}} \leq 10^{5.7} \text{ K}$ , and  $5 \text{ Mpc} \leq R_{\text{mfp}} \leq 40 \text{ Mpc}$ . See Mesinger et al. (2012), Pober et al. (2014), Greig & Mesinger (2015), and references therein for the rationale behind these ranges. Note that the  $R_{\text{mfp}}$  parameter roughly corresponds to a time-averaged mean

<sup>9</sup> In the literature on 21cmFAST, this parameter is often referred to as a mean free path for ionizing photons, but in actuality, it sets a sharp cutoff for the maximum distance an ionizing photon can travel before it is absorbed.

<sup>10</sup> While there are no direct measurements of the temperature of putative cosmic HI regions at this redshift, theoretical expectations are that X-ray heating from collapsed stellar remnants (Furlanetto 2006; McQuinn 2012; Mesinger et al. 2013) brings the spin temperature of the gas well above that of the CMB. Even in the absence of this mechanism, shock heating should be enough to raise the spin temperature above the CMB temperature at this low redshift (McQuinn & O’Leary 2012).

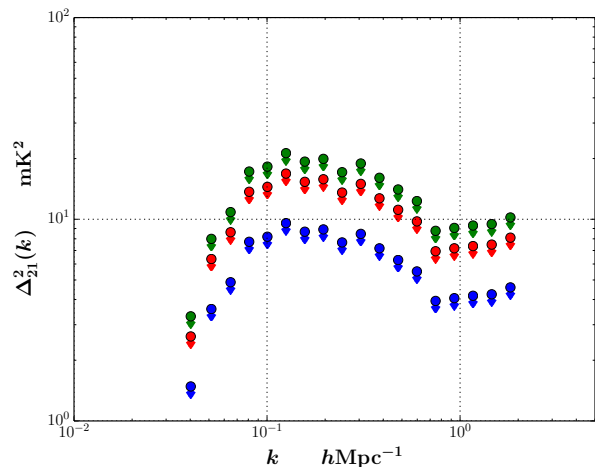


**Figure 1.** Confidence upper limits on the amplitude of the  $z = 5.9$  21 cm power spectrum as a function of  $k$ . Colors corresponds to 65 per cent confidence (blue), 95 per cent confidence (red), and 99 per cent confidence (green).

free path through the ionized IGM, and so is likely to be at or below the measurements at  $z \sim 6$  from, e.g., Songaila & Cowie (2010). We also note that the evolution and structure of reionization in the simulations is insensitive to this choice beyond  $R_{\text{mfp}} \gtrsim 30 \text{ Mpc}$  (see, e.g., Furlanetto & Mesinger 2009 and Alvarez & Abel 2012).

Figure 1 shows the main result of this paper: the upper limits on the 21 cm power spectrum amplitude as a function of  $k$ . We plot 65 per cent, 95 per cent, and 99 per cent confidence limits in blue, red, and green, respectively. In general, there is no significant variation in amplitude as a function of  $k$  and most limits are within a factor of two of  $10 \text{ mK}^2$ . While we do not plot the individual PDFs for each  $k$  mode, we note that they are one-sided Gaussian curves, with a peak at  $\Delta^2(k) = 0 \text{ mK}^2$ . The Gaussianity of the PDFs results from treating the McGreer et al. (2015) limits as Gaussian.

Comparison of these results with typical 21cmFAST outputs (e.g. Figure 4 of Pober et al. 2014) show that the shape of the limits with  $k$  is not surprising. The knee feature due to the finite extent of ionized bubbles exhibits itself as an absence of power on the largest scales, whereas the remaining  $k$  modes show a relatively flat power. The peak in large-scale power around  $k \sim 0.1 \text{ hMpc}^{-1}$  is set by models with highly biased sources (i.e. high  $T_{\text{vir,min}}$ ) and large values of  $R_{\text{mfp}}$ . This combination of parameters can result in large cosmic HI patches left over in the final stages of reionization. On the other hand, the fall off in power towards high  $k$  depends most strongly on the  $R_{\text{mfp}}$ . These constraints span a range in  $k$  from approximately  $0.05$  to  $2.0 \text{ hMpc}^{-1}$ , covering the region where first-generation 21 cm experiments will have maximal sensitivity (Parsons et al. 2012a,b; van Haarlem et al. 2013; Beardsley et al. 2013; Pober et al. 2014).

#### 4 DISCUSSION

The principal implications of this result are simple: 21 cm cosmology experiments should not detect power spectra above  $\sim 10 - 20 \text{ mK}^2$  at  $z = 5.9$ . A detection of power above this level would be highly indicative of residual foregrounds or other systematic contamination of the power spectrum. This test should be used in conjunction with other measurements at higher redshifts. That is to say, an experiment claiming a detection of cosmological power at  $z > 6.0$  would be suspect if it also detected power above this limit at  $z = 5.9$ .

To get a scale for this limit, we can compare it with both the current best limits on the 21 cm signal and with expected power spectrum amplitudes for the reionization signal. The current best limits on the 21 cm power spectrum come from Ali et al. (2015) at  $z = 8.4$ , constraining  $\Delta^2(k) < 501.8 \text{ mK}^2$  for  $0.15 \text{ hMpc}^{-1} < k < 0.5 \text{ hMpc}^{-1}$ . Limits from Jacobs et al. (2015) cover a range of other redshifts, including  $z = 7.55$ , but are over a factor of four above the Ali et al. (2015) limits. A significant increase in sensitivity over current limits is therefore needed to reach the theoretical limits presented here; however, the steep spectral slope of sky noise reduces the power spectrum noise level by a factor of nearly three from  $z = 8.4$  to  $5.9$  (assuming a spectrally flat receiver contribution of  $100 \text{ K}$ ). Most models, on the other hand, predict reionization power spectra with peak brightnesses of  $\sim 10 \text{ mK}^2$  (Pober et al. 2014; Mesinger et al. 2016), on par with the limits presented here. Therefore, with even a factor of two to three less integration time at  $z = 5.9$ , any 21 cm experiment presenting a detection result at higher redshift should have the sensitivity to compare with the results presented here.

Estimates for the amount of integration time needed to make a first detection of the 21 cm signal with current experiments range from several hundred to one-thousand hours (Morales 2005; McQuinn et al. 2006; Pen et al. 2009; Parsons et al. 2012a; Beardsley et al. 2013; van Haarlem et al. 2013; Pober et al. 2014). Therefore, even a factor of three less observing time for a null result at  $z = 5.9$  is a significant investment of resources. For experiments with very wide instantaneous bandwidths,  $z = 5.9$  measurements come in effect “for free.” Unfortunately, none of the first generation experiments are quite able to achieve this. The PAPER experiment has an instantaneous bandwidth from 100 to 200 MHz ( $z = 6.1$  to  $z = 13.2$ ), with a somewhat smaller usable bandwidth due to analog filters and the difficulty of foreground removal near the end of the band (Parsons et al. 2010). The MWA is sensitive to frequencies between 80 and 300 MHz ( $z = 3.7$  to  $z = 16.8$ ), and so can easily target a redshift of 5.9; however, it has an instantaneous bandwidth of only 30.72 MHz, and so would need to devote a separate observing campaign for the  $z = 5.9$  limit. Depending on the Nyquist zone chosen, LOFAR high band antennae have an instantaneous bandwidth covering either 110 to 190 MHz ( $z = 6.5$  to  $z = 11.9$ ), 170 to 230 MHz ( $z = 5.2$  to  $z = 7.4$ ), or 210 - 250 MHz ( $z = 5.2$  to  $z = 5.8$ ) (van Haarlem et al. 2013). While either of the latter two modes would allow for a  $z = 5.9$  test, it appears that most of LOFAR’s EoR observing has taken place in the first mode (Yatawatta et al. 2013; Jelić et al. 2014). Next generation experiments like the

Hydrogen Epoch of Reionization Array (HERA)<sup>11</sup> and the Square Kilometre Array (SKA)<sup>12</sup> are being designed with wider instantaneous bandwidths and so can take advantage of this low redshift limit without devoting additional observing time. HERA, in particular, is targeting an instantaneous bandwidth of 50 – 250 MHz (DeBoer et al., *in prep.*); taking into account the sensitivities for HERA calculated in DeBoer et al., *in prep.*, HERA should not only be able to use the upper limits here as a consistency check on its higher redshift measurements, but should also be able to detect the presence of neutral gas in the IGM below  $z = 6$  with high significance.

Lastly, it is worth commenting on the uncertainties introduced in this calculation through our dependence on 21cmFAST models of reionization. The three parameter ( $\zeta$ ,  $T_{\text{vir,min}}$ ,  $R_{\text{mfp}}$ ) model for reionization is certainly simplified, although as we note above, it nevertheless serves to provide an effective basis set for 21 cm power spectra. One significant approximation is that does not include any time or halo mass dependence in the parameters. For this work, however, the lack of spatial fluctuations in the ionizing photon mean free path can be considered the poorest approximation. The end stages of reionization can be highly sensitive to the interplay between sources and sinks of ionizing photons, producing non-trivial spatial inhomogeneities that are not captured by a uniform photon horizon (e.g. Sobacchi & Mesinger 2014). However, we note that more realistic models (e.g. Mesinger et al. 2016) predict significantly less 21 cm power on moderate and large scales during the end of reionization. In particular, the two reionization simulations in Mesinger et al. (2016) produce 21 cm power spectra with maximum values of  $\sim 2$  and  $\sim 7 \text{ mK}^2$  (depending on the bias of the galaxies responsible for the ionizing photons) when the universe is 10 to 15 per cent neutral. In this sense, our limits on the 21 cm signal are conservative; including more physics in the simulations would further reduce the probability of a bright 21 cm signal at  $z = 5.9$ .

The EoR morphology of Sobacchi & Mesinger (2014) can be crudely approximated by a small photon horizon. Lowering the  $R_{\text{mfp}}$  prior therefore should reproduce the general trend expected from more realistic reionization simulations. If we limit the range of  $R_{\text{mfp}}$  to less than 15 Mpc, our two and three sigma upper limits at  $k \lesssim 0.2 \text{ hMpc}^{-1}$  decrease by a factor of  $\sim 2$ , with limits at higher  $k$  effectively unchanged, again suggesting that our overall limits are conservative.

We have also neglected to incorporate evolution effects across the redshift axis of our 21cmFAST simulations, i.e., the light cone effect (Datta et al. 2012, 2014; La Plante et al. 2014). Investigations into this effect find the largest scales of the 21 cm power spectrum to be the most affected ( $k \lesssim 0.1 \text{ hMpc}^{-1}$ ), which are those most likely to be contaminated by foregrounds for the current and next generation of 21 cm experiments (Parsons et al. (2012a); Pober et al. (2014); Sims et al., *in review*). More importantly, the general trend of the effect during the end of reionization is reduce power on the larger scales by tens of per cent (Datta et al. 2014).

<sup>11</sup> <http://reionization.org>

<sup>12</sup> <http://skatelescope.org>



Therefore, in this regard, our upper limits on the 21 cm signal are conservatively high.

## 5 CONCLUSIONS

We have presented an upper limit on the amplitude of the 21 cm power spectrum at a redshift of 5.9. This limit is derived from the model-independent limit on the neutral fraction from the dark pixel analysis of quasar absorption spectra in [McGreer et al. \(2015\)](#). To convert a neutral fraction limit to a 21 cm power spectrum one, we use a modified version of 21CMMC to explore the likelihood of 21 cm power spectra given the prior constraints. The end result is a limit of  $\Delta^2(k) < 10$  to 20 mK<sup>2</sup> at 99 per cent confidence, over a range of  $k$  from roughly 0.5 to 2.0  $h\text{Mpc}^{-1}$ , with the exact value depending on the  $k$  mode in question. This limit can be used as a null test for 21 cm experiments looking to build confidence in any purported initial detection of the cosmological signal. While a non-detection of power at these redshifts is not definitive validation of a higher redshift detection, any power detected at  $z = 5.9$  in excess of our limit is highly suggestive of residual foregrounds or systematic errors that would likely also affect measurements at other redshifts.

## ACKNOWLEDGEMENTS

The authors would like to thank Steve Furlanetto and James Aguirre for helpful comments on a draft version of this manuscript. AM and BG acknowledge support from the European Research Council (ERC) under the European Union's Horizon 2020 research and innovation program (Starting Grant No. 638809 — AIDA — PI: Mesinger).

## REFERENCES

- Ali Z. S., et al., 2015, [ApJ](#), **809**, 61
- Alvarez M. A., Abel T., 2012, [ApJ](#), **747**, 126
- Ansari R., et al., 2012, [A&A](#), **540**, A129
- Barkana R., Loeb A., 2007, [Reports on Progress in Physics](#), **70**, 627
- Beardsley A. P., et al., 2013, [MNRAS](#), **429**, L5
- Bittner J. M., Loeb A., 2011, [Journal of Cosmology and Astroparticle Physics](#), **4**, 38
- Crociani D., Mesinger A., Moscardini L., Furlanetto S., 2011, [MNRAS](#), **411**, 289
- Datta K. K., Mellema G., Mao Y., Iliev I. T., Shapiro P. R., Ahn K., 2012, [MNRAS](#), **424**, 1877
- Datta K. K., Jensen H., Majumdar S., Mellema G., Iliev I. T., Mao Y., Shapiro P. R., Ahn K., 2014, [MNRAS](#), **442**, 1491
- Dillon J. S., et al., 2015, [Phys. Rev. D](#), **91**, 123011
- Fernandez E. R., Zaroubi S., Iliev I. T., Mellema G., Jelić V., 2014, [MNRAS](#), **440**, 298
- Furlanetto S. R., 2006, [MNRAS](#), **371**, 867
- Furlanetto S. R., Lidz A., 2007, [ApJ](#), **660**, 1030
- Furlanetto S. R., Mesinger A., 2009, [MNRAS](#), **394**, 1667
- Furlanetto S. R., Zaldarriaga M., Hernquist L., 2004, [ApJ](#), **613**, 16
- Geil P. M., Mutch S. J., Poole G. B., Angel P. W., Duffy A. R., Mesinger A., Wyithe J. S. B., 2015, preprint, ([arXiv:1512.00564](#))
- Gong Y., Cooray A., Silva M. B., Santos M. G., Lubin P., 2011, [ApJ](#), **728**, L46
- Gong Y., Cooray A., Silva M., Santos M. G., Bock J., Bradford C. M., Zemcov M., 2012, [ApJ](#), **745**, 49
- Greig B., Mesinger A., 2015, [MNRAS](#), **449**, 4246
- Greig B., Mesinger A., Pober J. C., 2016, [MNRAS](#), **455**, 4295
- Jacobs D. C., et al., 2015, [ApJ](#), **801**, 51
- Jelić V., et al., 2014, [A&A](#), **568**, A101
- La Plante P., Battaglia N., Natarajan A., Peterson J. B., Trac H., Cen R., Loeb A., 2014, [ApJ](#), **789**, 31
- Lidz A., Zahn O., McQuinn M., Zaldarriaga M., Hernquist L., 2008, [ApJ](#), **680**, 962
- Lidz A., Furlanetto S. R., Oh S. P., Aguirre J., Chang T.-C., Doré O., Pritchard J. R., 2011, [ApJ](#), **741**, 70
- Mao X.-C., 2014, [ApJ](#), **790**, 148
- McGreer I. D., Mesinger A., D'Odorico V., 2015, [MNRAS](#), **447**, 499
- McQuinn M., 2012, [MNRAS](#), **426**, 1349
- McQuinn M., O'Leary R. M., 2012, [ApJ](#), **760**, 3
- McQuinn M., Zahn O., Zaldarriaga M., Hernquist L., Furlanetto S. R., 2006, [ApJ](#), **653**, 815
- Mesinger A., Furlanetto S., 2007, [ApJ](#), **669**, 663
- Mesinger A., Furlanetto S., Cen R., 2011, [MNRAS](#), **411**, 955
- Mesinger A., McQuinn M., Spergel D. N., 2012, [MNRAS](#), **422**, 1403
- Mesinger A., Ferrara A., Spiegel D. S., 2013, [MNRAS](#), **431**, 621
- Mesinger A., Greig B., Sobacchi E., 2016, [MNRAS](#), **459**, 2342
- Morales M. F., 2005, [ApJ](#), **619**, 678
- Parsons A. R., et al., 2010, [AJ](#), **139**, 1468
- Parsons A., Pober J., McQuinn M., Jacobs D., Aguirre J., 2012a, [ApJ](#), **753**, 81
- Parsons A. R., Pober J. C., Aguirre J. E., Carilli C. L., Jacobs D. C., Moore D. F., 2012b, [ApJ](#), **756**, 165
- Parsons A. R., et al., 2014, [ApJ](#), **788**, 106
- Pen U.-L., Chang T.-C., Hirata C. M., Peterson J. B., Roy J., Gupta Y., Odegova J., Sigurdson K., 2009, [MNRAS](#), **399**, 181
- Planck Collaboration et al., 2015, preprint, ([arXiv:1502.01589](#))
- Pober J. C., 2015, [MNRAS](#), **447**, 1705
- Pober J. C., et al., 2013, [AJ](#), **145**, 65
- Pober J. C., et al., 2014, [ApJ](#), **782**, 66
- Pober J. C., et al., 2015, [ApJ](#), **809**, 62
- Sobacchi E., Mesinger A., 2014, [MNRAS](#), **440**, 1662
- Sobacchi E., Mesinger A., Greig B., 2016, [MNRAS](#), **459**, 2342
- Songaila A., Cowie L. L., 2010, [ApJ](#), **721**, 1448
- Swarup G., Ananthakrishnan S., Kapahi V. K., Rao A. P., Subrahmanya C. R., Kulkarni V. K., 1991, [Current Science](#), Vol. 60, NO.2/JAN25, P. 95, 1991, **60**, 95
- Tingay S. J., et al., 2013, [Publications of the Astronomical Society of Australia](#), **30**, 7
- Trott C. M., et al., 2016, [ApJ](#), **818**, 139
- Vrbanec D., et al., 2016, [MNRAS](#), **457**, 666
- Wyithe J. S. B., Loeb A., Schmidt B. P., 2007, [MNRAS](#), **380**, 1087
- Yatawatta S., et al., 2013, [A&A](#), **550**, A136
- Zel'dovich Y. B., 1970, [A&A](#), **5**, 84
- van Haarlem M. P., et al., 2013, [A&A](#), **556**, A2

This paper has been typeset from a  $\text{\LaTeX}$  file prepared by the author.